Turkish Journal of Electrical Engineering & Computer Sciences

http://journals.tubitak.gov.tr/elektrik/

Research Article

Turk J Elec Eng & Comp Sci
(2014) 22: 1410 – 1422

doi:10.3906/elk-1201-70

Implementation of neural network-based maximum power tracking control for wind turbine generators

Abdulhakim KARAKAYA*, **Ercüment KARAKAŞ**
Department of Electrical Education, Kocaeli University, İzmit, Turkey

Received: 22.01.2012 • **Accepted:** 24.05.2012 • **Published Online:** 07.11.2014 • **Printed:** 28.11.2014

Abstract: In this study, the maximum power point tracking (MPPT) of a permanent magnet synchronous generator used in a wind generator system is realized by a prototype installed in a laboratory environment. The installed prototype is modeled in a MATLAB/Simulink environment. The MPPT is realized by an artificial neural network (ANN). The obtained simulation and experimental results are compared. The maximum power estimation at various windmill speeds (rpm) of the trained ANN in determined reference speeds is analyzed. The zero crossing points of the phases are determined by a digital signal peripheral interface controller and the system is operated according to the triggering angles obtained from the ANN-based control algorithm at the maximum power points.

Key words: Maximum power point tracking, permanent magnet synchronous generator, artificial neural network control, wind energy

1. Introduction

Renewable energy sources are gaining attention due to global warming and greenhouse effects. A part of the globally demanded energy can be produced by wind energy as one of the important forms of these sources. Many national and international works are performed in order to produce the maximum power from wind energy. Permanent magnet synchronous generators (PMSGs) are attracting great attention among these works because PMSGs are driven directly and they satisfactorily perform in a wide range of wind speeds. Wind energy is facilitated optimally by tracking the maximum power of the wind turbines and the maximum aerodynamic efficiency can be obtained [1]. The generator is operated at variable speed and frequency modes in order to track the maximum power point. Anemometers are used in order to vary the generator speed, driven by the desired shaft speed, and measure the wind speed in many designed controllers in the literature [2].

Studies on the maximum power point tracking (MPPT) of PMSGs using artificial neural networks (ANNs) have been mostly simulation-dominated in recent years [2–7]. A simulation study was accomplished for the wind speed estimation and tracking control of the optimal maximum power based on a turbine power factor curve against the potential drift for a small-size ANN-using wind system in [2]. It can be seen that not only the MPPT but also the output voltage regulation of the wind turbine may have been accomplished using an ANN for a PMSG system based on the simulation results in [3]. The maximum power tracking performance analysis was presented at various wind speeds based on the simulation of the wind speed prediction by the ANN in [4]. The simulation results were analyzed by wind speed prediction using a Jordan-type ANN in [5]. An analysis of

*Correspondence: abdkarakaya@hotmail.com

the simulation results related to the control of the proposed voltage frequency controller by the ANN, which is based on the adaptive linear element approach, was presented in [6]. Results related to the wind and rotor speed estimation using a nonlinear autoregressive moving average ANN model were analyzed in [7]. However, many MPPT control algorithms related to PMSGs were used in [8–19]. In this study, not only a simulation but also an experiment is accomplished. The obtained results are compared and analyzed. It is presented that MPPT can be performed using the addition of a simple algorithm. The ANN-controlled MPPT is accomplished by installed a prototype in a laboratory environment. The hands-on training of the PMSG, which is an important part of renewable energy systems, is delivered to students using this prototype. The analysis of the maximum power estimation for the different rotor speeds of the ANN trained in the reference speeds is accomplished. The zero-crossing points of the phases are determined by a digital signal peripheral interface controller (dsPIC) and the system is operated according to the triggering angles obtained from the ANN-based control algorithm at the maximum power points. MPPT can be accomplished easily without any necessity for the anemometer or the sensor, owing to the determination of the phase angles by the dsPIC program.

2. Wind turbine generator system

The mechanical input power captured by the wind turbine is given in Eq. (1).

$$P_m = 0.5\rho A V_w^3 C_p \tag{1}$$

Here, ρ is the air density (kg/m^3), A is the swept area (m^2), Cp is the power coefficient of the wind turbine, and V_w is the wind speed (m/s).

In Eq. (1), if the wind speed, air density, and swept area are stable and fixed, the output power of the turbine will be a function of the power coefficient. Moreover, the wind turbine is a characteristic of the $C_{p-\lambda}$ curve, where λ is the tip-speed ratio, which is given in Eq. (2).

$$\lambda = \frac{\omega_{rm} R}{V_w} \tag{2}$$

Here, R is the radius of the blades and ω_m is the rotational speed of the wind turbine shaft. In Figure 1, there is a $C_{p-\lambda}$ curve for the wind turbine. As shown in Figure 1, the C_p has a value of Cpmax, which is the optimum point at λ_{opt}. The maximum mechanical power should change depending on the rotational speed of the windmill and the wind speed. The relation between the windmill speed and the output power according to the wind speed change and P_{max} versus the rpm at different wind speeds is shown in Figure 2.

3. Mathematical model of the PMSG

Figure 3 shows a simulation block diagram of the proposed system. The model is established using MATLAB/Simulink blocks. The DC motor speed is controlled by a PID according to the reference speed. The produced voltage by the PMSG, which is coupled to the DC motor, is rectified by thyristors. The ANN controller produces the maximum power angles according to the DC motor speed (PMSG speed) and the thyristors are triggered according to these angles. The obtained V_{dc} voltage is filtered by a capacitor (C = 1500 μF) and is supplied into the R_L load.

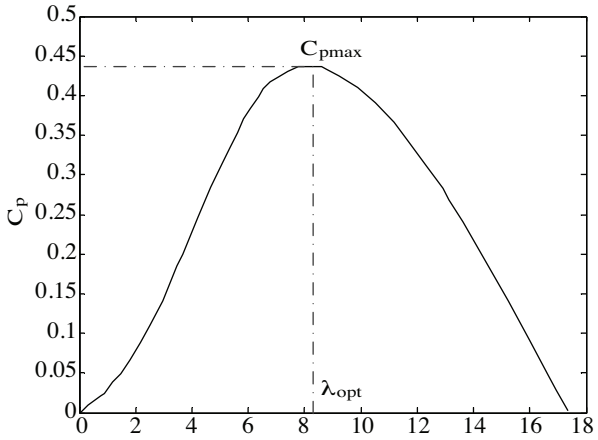

Figure 1. Power coefficient versus the tip speed ratio.

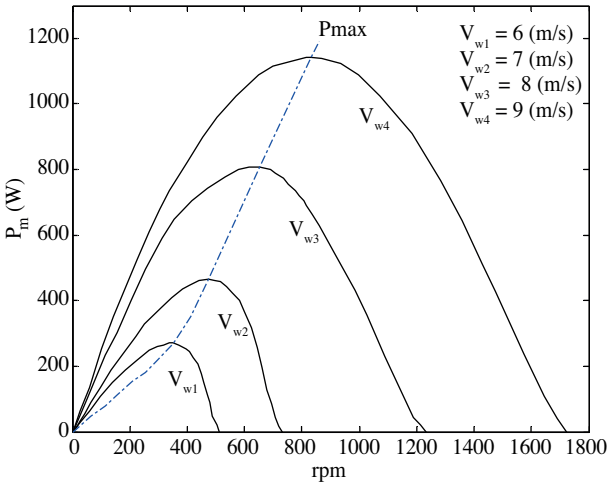

Figure 2. Relationship between the power and the windmill speed.

The voltage and electromagnetic torque equations for the PMSG in the d-q axis synchronous rotational reference frame can be expressed as follows [20,21]:

$$v_q = -r_s\, i_q - \frac{d\,(\lambda_q)}{dt} + \omega_r\, \lambda_d, \tag{3}$$

$$v_d = -r_s\, i_d - \frac{d\,(\lambda_d)}{dt} - \omega_r\, \lambda_q, \tag{4}$$

$$\lambda_d = L_d\, i_d + \lambda_m, \tag{5}$$

$$\lambda_q = L_q\, i_q, \tag{6}$$

$$T_e = \frac{3}{2}\,\frac{P}{2}\,[\,(L_d - L_q)\, i_d\, i_q + \lambda_m\, i_q\,], \tag{7}$$

$$\omega_r = \frac{P}{2}\,\omega_{rm}, \tag{8}$$

$$\omega_{rm} = \frac{2\,\pi\, n}{60}, \tag{9}$$

where V_d and V_q represent the d-q axes voltages, i_d and i_q are the d-q axis currents, L_d and L_q are the d-q axis inductances, r_s is the per phase stator resistance, ω_r shows the electrical velocity of the rotor, λ_m is the expression of the flux linkage due to the rotor magnets linking the stator, T_e is the electromagnetic torque, n is the rotor shaft speed (rpm), and ω_{rm} is the mechanical velocity of the rotor.

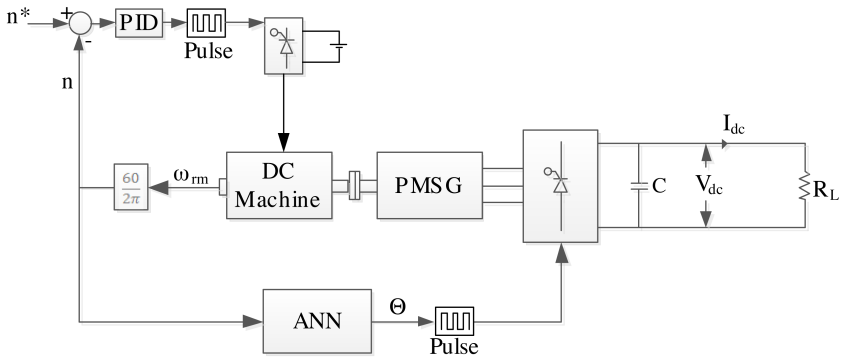

Figure 3. The simulation block diagram of the proposed system.

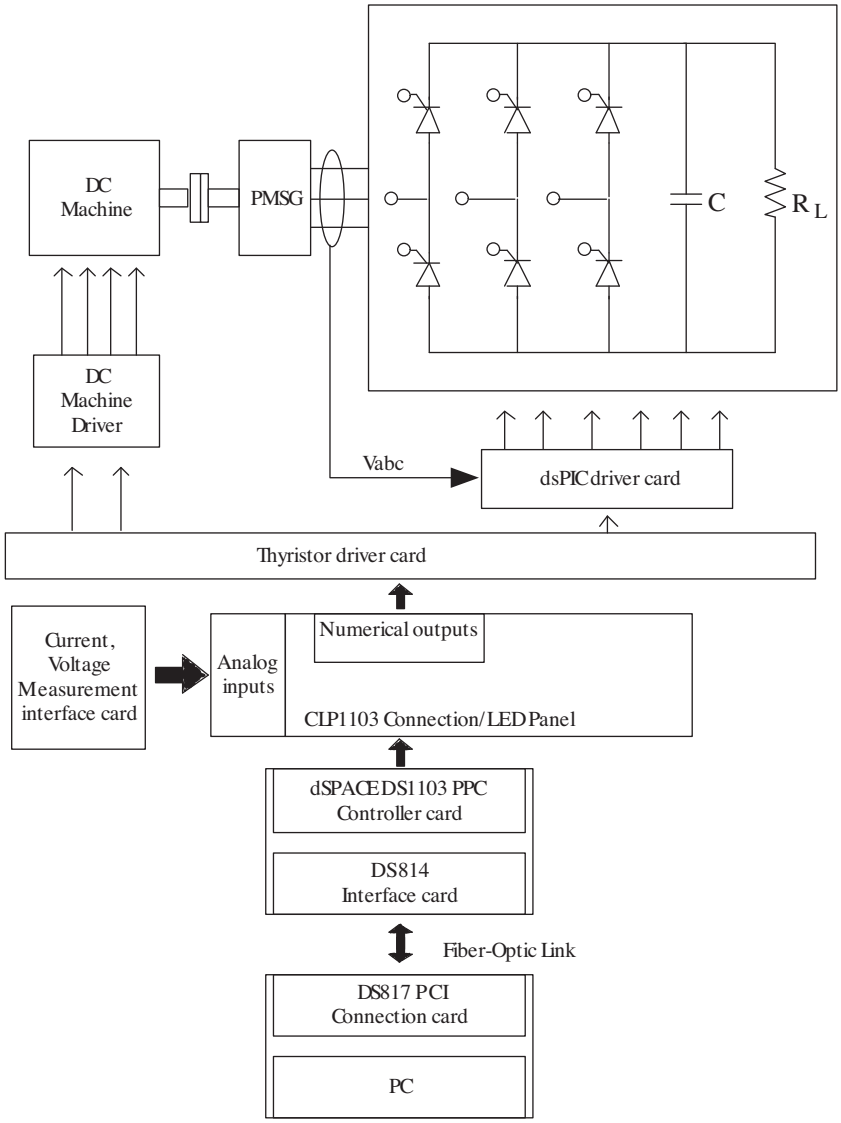

Figure 4. The experimental block diagram of the proposed system.

4. Maximum power tracking control system

4.1. System description

As shown in Figure 4, the DC motor is coupled to the PMSG. The PMSG is operated by the DC motor. A 3-phase AC voltage produced by the PMSG is converted to DC voltage by means of the thyristors and is filtered by the capacitor. The converted voltage is supplied to the DC load. The MathWorks MATLAB/Simulink/real-time workshop and dSPACE Real-Time Interface (RTI) and ControlDesk software are used in order to control the dsPIC driver. The RTI and ControlDesk software presented by dSPACE are facilitated in order to accomplish the experiment and collect the data in real time. The RTI is realization software that is used in order to run the Simulink models on the hardware without any programming. The ControlDesk software of dSPACE is facilitated in order to record, analyze, and investigate the experimental data.

A general-purpose thyristor driver circuit block diagram is seen in Figure 5. A dsPIC30f4011 digital signal controller is the core for the motor control applications developed by Microchip. It is a 30-MHz, 16-bit architecture, high-performance, low-cost controller, which has all of the features of the motor controller family, with an ADC and PWM interface with high resolution. The reference signals taken from the V_a, V_b, and V_c phases are isolated by optoisolators and the zero-crossing signals are obtained according to the source voltage. The timing of the thyristor triggering is determined via a synchronous zero-crossing signal. The operation mode of the thyristor driver, digital or analog, is selected by a switch. In this study, the digital mode is selected. The switching signals are delivered to the thyristors at maximum power points.

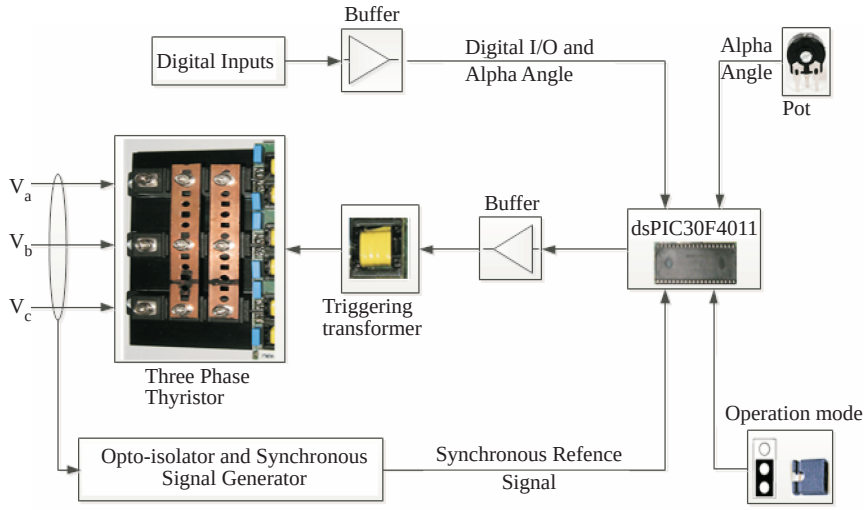

Figure 5. The block diagram of the thyristor driver.

The thyristor driver card is designed based on the dsPIC30F4011 microcontroller for a general purpose and can be operated in 3 different cases, as 3-phase or 1-phase full-controlled rectifier, 3-phase or 1-phase AC voltage controller, or 3-phase or 1-phase static switch [22]. In this paper, the multipurpose card was designed by Kesler et al. [22]. The dsPIC software is updated in order to be used as the 3-phase rectifier for the wind generator systems. A snapshot of the designed thyristor driver card is shown in Figure 6.

4.2. Maximum power tracking control scheme

The methods for the maximum power tracking are as follows. The block diagram of the system shown in Figure 4 is applied for the determination of the maximum power points. The pole winding of the DC shunt motor is

supplied by a full-wave DC voltage (200 V). The armature voltage is adjusted in order to control the motor speed by the controlled thyristor rectifier. The PMSG is excited by a DC motor. The maximum power points (P_{max}) are obtained by changing the switching angles for each of the windmill speeds, as in Figure 2. The maximum power data according to the experimental results are shown in Table 1.

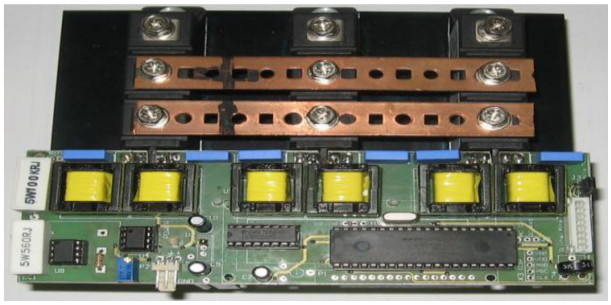

Figure 6. Thyristor driver card.

Table 1. Maximum power data according to the shaft speed.

n (rpm)	Obtained P_{max} (W)	n (rpm)	Obtained P_{max} (W)
150	21.566	475	467.56
175	51.248	500	510.129
200	69.174	525	562.771
225	103.902	550	609.367
250	123.132	575	670.982
275	147.246	600	738.321
300	177.244	625	786.872
325	209.907	650	835.212
350	249.821	675	874.433
375	288.084	700	925.904
400	328.431	725	975.106
425	370.781	750	1030.674
450	413.253		

The ANN is trained according to the 13 experimental data in Table 2 and MPPT is done. The thyristors are switched according to the windmill speed at the maximum power points.

4.3. ANN controlling model

The estimating algorithm of the thyristor switching angle proposed in this paper is based on a 2-D nonlinear inverse function, which is described in Figure 7. Tan and Islam [23] applied a 2-D lookup table of the power coefficient and power-mapping method to estimate the wind velocity directly or indirectly. The application of an inverse function by a 2-D lookup table is complex. This complexity increases the calculation time and reduces the performance. The usage of an ANN is an appropriate technique in order to solve this problem.

An ANN controller is used to precisely determine the maximum power points. The proposed training scheme for the prediction of the thyristor triggering angles of the ANN is seen in Figure 7. The shaft speed and corresponding thyristor triggering angles are seen in Table 2. The rpm samples are used as targets to train a 4-layer network, as shown in Figure 8, with 1 linear neuron in the input layer, 8 tan-sigmoid neurons in the first hidden layer, 3 tan-sigmoid neurons in the second hidden layer, and 1 linear neuron in the output layer. The

input network parameter windmill speed is n (rpm) and the output network parameter is a switching angle of θ (degrees). The training operation is made in 200 cycles using 13 input-output patterns, as shown in Table 2.

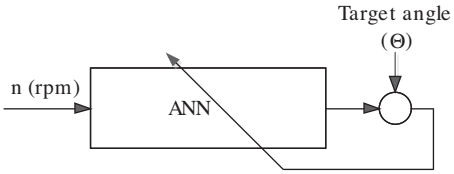

Figure 7. Proposed training scheme for the ANN-based thyristor switching angle estimation.

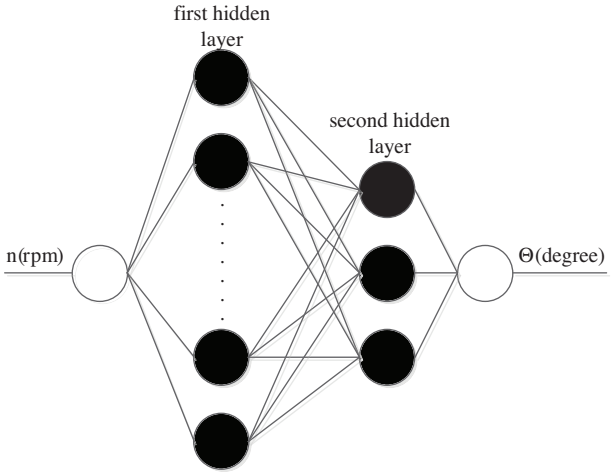

Figure 8. Structure of the ANN.

Table 2. Data used in the ANN training and test.

Data used in the training		Data used in the ANN test	
n (rpm)	θ (degree)	n (rpm)	θ (degree)
150	91	175	86
200	80	225	76
250	72	275	67
300	61	325	53
350	46	375	38
400	34	425	30
450	25	475	19
500	17	525	13
550	11	575	8
600	2	625	2
650	2	675	2
700	2	725	2
750	2		

Offline training is applied for the suggested ANN controller. Offline data can be obtained by simulation or experiments. The data for this study are obtained at the end of the experimental results. The DC motor shaft is rotated at different 25 speeds. The triggering angles of the thyristors are obtained based on the trial and error method in order to obtain the maximum power according to the adjusted reference shaft speed of the PMSG. The application results are given in Table 2. The maximum power tracking is accomplished by the ANN-trained 13 input-output data in Table 2.

4.4. Experimental results

The simulation and experimental diagram of the system is shown in Figures 3 and 4, respectively. The experimental set photo is shown in Figure 9. The application set is our own design. The set is placed onto

an aluminum sled with 360° swivel wheels in order to be carried to the desired location. A 1-kW PMSG and 2.2-kW DC motor are coupled by centering. All of the DC motor and PMSG ports are cabled to external connectors in order to ease the connection. The 3-phase voltage produced by the generator is fed to the control unit. The control unit can measure all of the currents and voltages of the PMSG and DC bus. Moreover, the zero-crossing angles of the phases are determined by the dsPIC rectifier card. The designed unit is removable from the sled seen in the Figure 9; hence, it can be used for other applications.

The controlling algorithm and maximum power tracking control are verified by the experimental results. The necessary parameters for the simulation of the PMSG are shown in the Table 3. They were obtained as in [24].

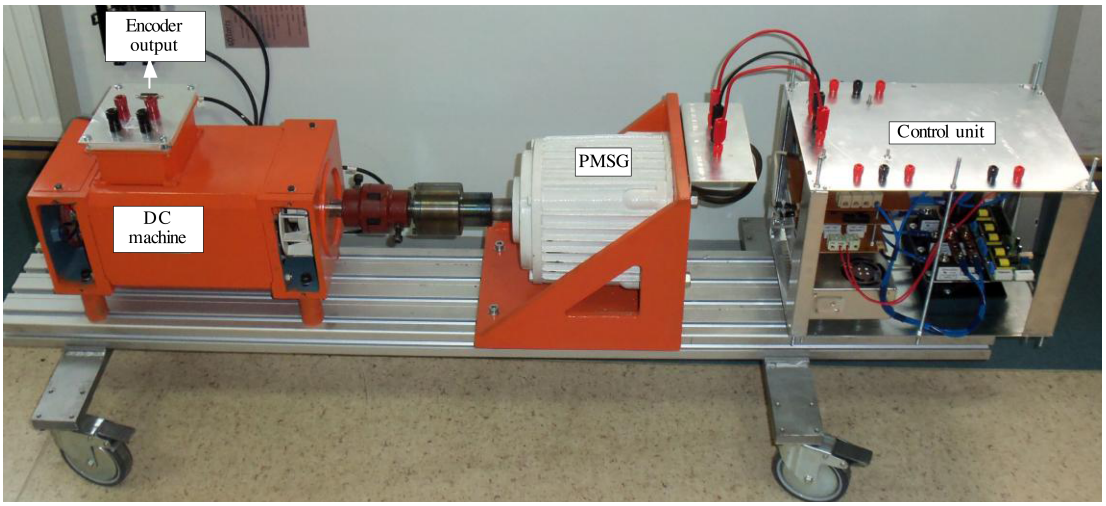

Figure 9. Experimental set.

A wind turbine is simulated by the DC motor. In a real wind generator system, the operation speed shows the characteristics related to the change in the load torque. However, considering only the load torque is not enough in the simulation system and the wind turbine can only be simulated by the speed control in simulation. For this reason, the operation of the generator is tested at the reference speeds. These tests are accomplished in the range of 150–750 rpm. It is determined that the thyristors must be triggered according to 25 different angles, corresponding to different speeds, in order to track the maximum power point shown in Table 2. The obtained MPPT data from the PMSG at the end of the application, according to Table 2, are shown in Table 1.

A trained ANN controller is analyzed by 12 test data in Table 2 using MATLAB/Simulink. The obtained results are given in Table 4. The application and simulation results are given in Tables 1 and 4, respectively, and the changing of these applications are seen in Figure 10. The ANN controller accomplished the maximum power transfer with a 0.17% error according to the analyzed results seen in Table 4.

The windmill is spun at 3 different speeds (350, 525, and 725 rpm) by the DC motor in Figures 11 and 12. The obtained maximum power at these speeds from the PMSG is consumed by the R_L load in Figure 4. The application and simulation results for the power (P_{max}), current (I_{dc}), and voltage (V_{dc}), and the changing of the 3-phase voltage (V_{abc}) and draw current (I_{abc}) from the PMSG can be seen in Figures 11 and 12, respectively.

Table 3. Parameters of the PMSG.

P (pairs of pole)	8
r_s (Ω)	1.35
L_d (mH)	5.893
L_q (mH)	7.967
λ_m (Wb)	0.3937
B (Nm/(rad/s))	1.25
J (kg/m^2)	0.0095

Table 4. ANN test results.

n (rpm)	Estimated degree (θ) by the ANN	Obtained P_{max} (W)
175	86	51.248
225	76	103.902
275	67	147.246
325	53	209.907
375	40	283.74
425	30	370.781
475	19	467.56
525	15	559.922
575	8	670.982
625	2	786.872
675	2	874.433
725	2	975.106

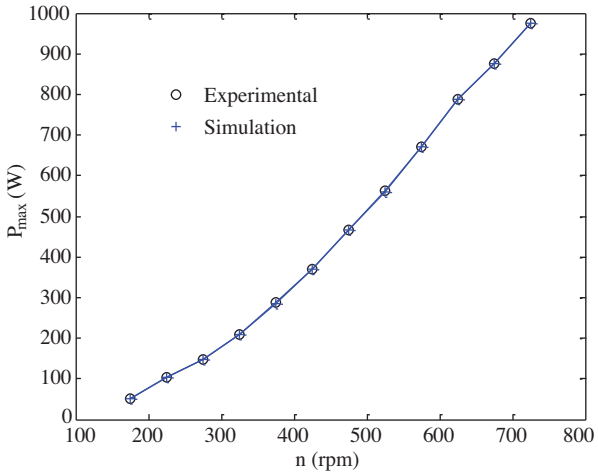

Figure 10. Application and simulation results of the maximum power change according to the windmill speed.

The PMSG shaft is spun at 525 rpm in Figures 13, 14, 15, and 16. The produced power of the PMSG is consumed at a 43-Ω R_L load in Figures 13 and 14, and at a 21-Ω R_L load in Figures 15 and 16. The application and simulation results of both the consumed power (P_{max}) in the R_L, the current (I_{dc}), and the voltage (V_{dc}), and the changing of the 3-phase voltage (V_{abc}) and draw current (I_{abc}) from PMSG can be seen in Figures 13 and 15, and Figures 14 and 16, respectively.

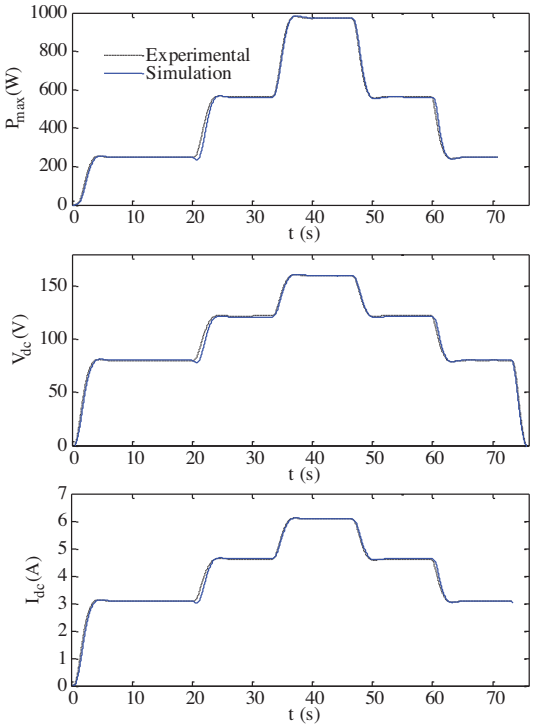

Figure 11. Application and simulation results of P_{max}, V_{dc}, and I_{dc} at the various windmill speeds (350, 525, and 725 rpm).

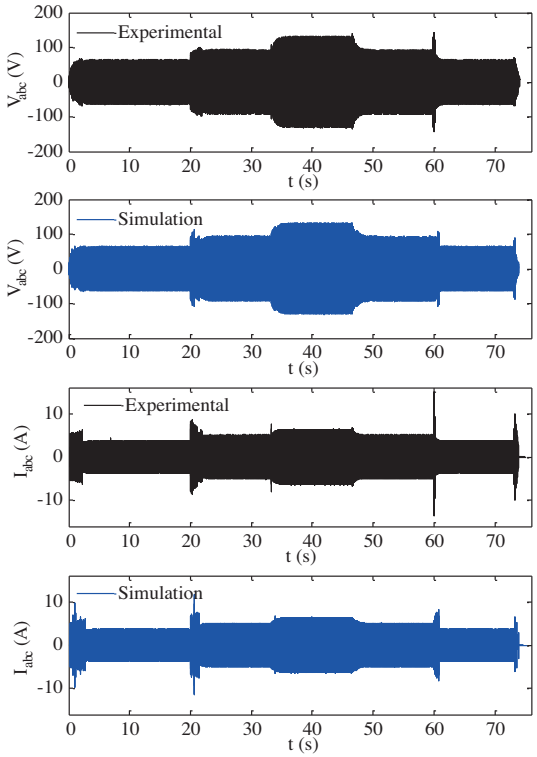

Figure 12. Application and simulation results of V_{abc} and I_{abc} at the various windmill speeds.

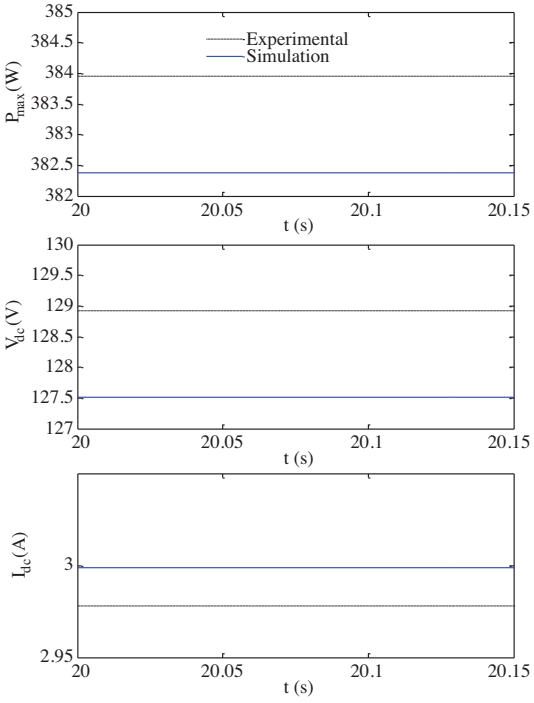

Figure 13. Application and simulation results of P_{max}, I_{dc}, and V_{dc} for 525 rpm at 43 Ω.

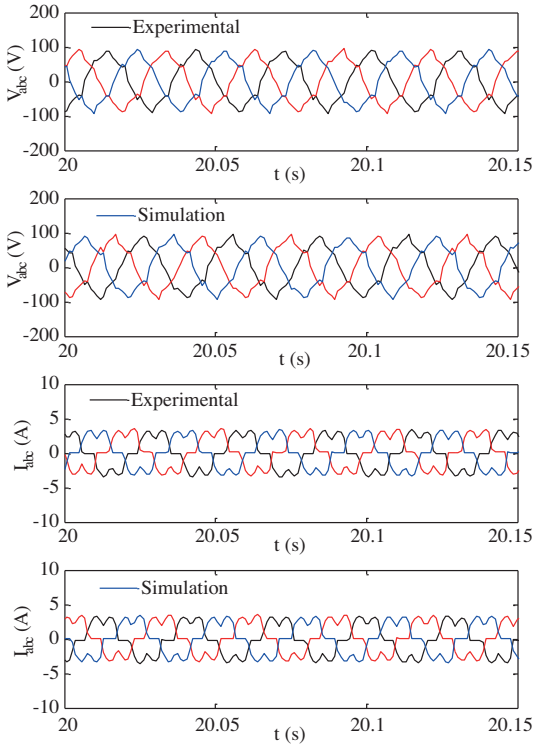

Figure 14. Application and simulation results of V_{abc} and I_{abc} for 525 rpm at 43 Ω.

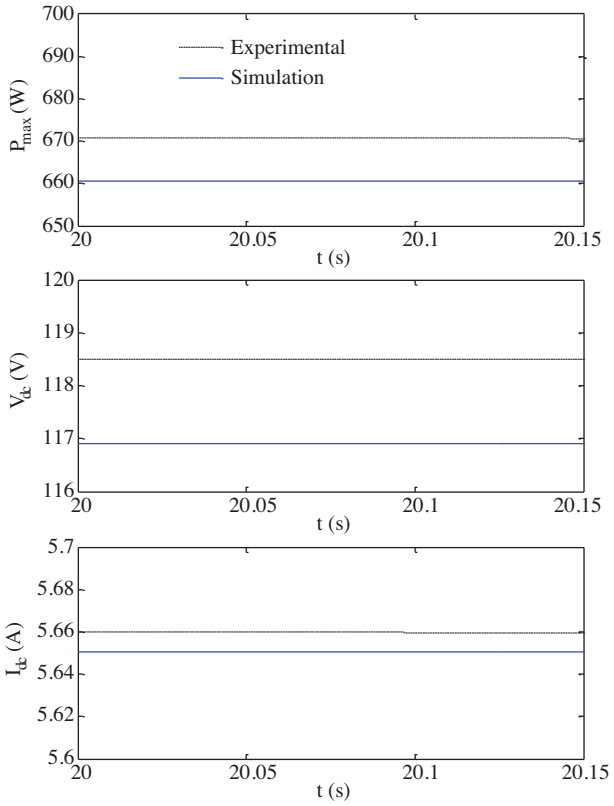

Figure 15. Application and simulation results of P_{max}, I_{dc}, and V_{dc} for 525 rpm at 21 Ω.

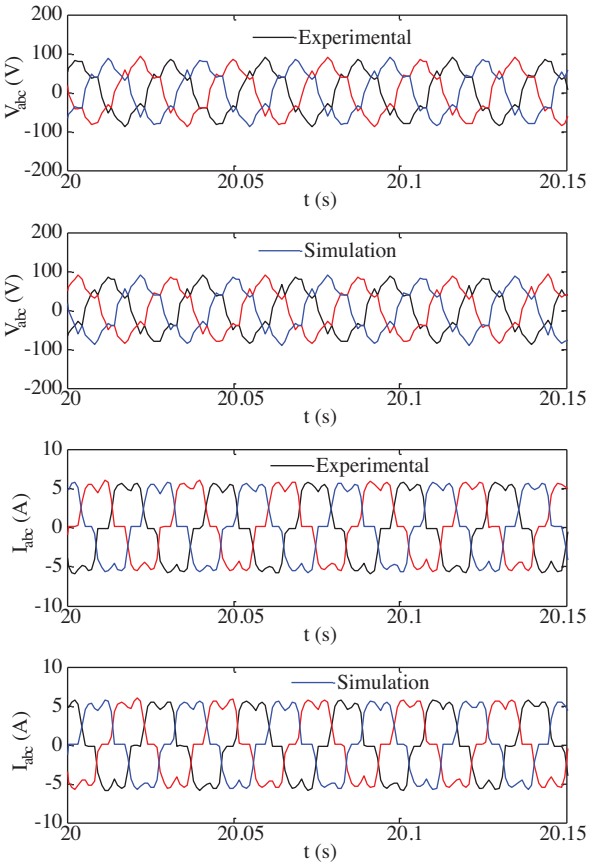

Figure 16. Application and simulation results of V_{abc} and I_{abc} for 525 rpm at 21 Ω.

5. Conclusion

In this study, an ANN controller was tested for a wind energy transformation system, in which a 1-kW PMSG was used. The performance of the ANN controller was tested according to the experimental and simulation results. It was aimed to accomplish MPPT with minimum error using a simple control strategy without any necessity for complicated mathematical manipulation. For this reason, an ANN was used for the MPPT of the PMSG. A control algorithm similar to a virtual environment was realized in the laboratory by a prototype and the results were analyzed. Power tracking can be performed with a 0.17% error according to the results of the simulation and application. The PMSG can easily be analyzed in a laboratory environment by the designed prototype. Hence, new MPPT strategies can be applied in order to make a contribution to the literature related to the PMSG, which is an important part of renewable energy sources. Additionally, the installed set can be used for educational purposes in educational foundations and student interest can be increased for renewable energy sources. The theoretical background of the students can be reinforced.

Acknowledgments

This work was supported by the Kocaeli University Scientific Research Project Center (Grant No. 2010/015).

References

[1] A.M. De Broe, S. Drouilhet, V. Gevorgian, "A peak power tracker for small wind turbines in battery charging applications", IEEE Transactions on Energy Conversion, Vol. 14, pp. 1630–1635, 1999.

[2] L.I. Hui, K.L. Shi, P.G. McLaren, "Neural-network-based sensorless maximum wind energy capture with compensated power coefficient", IEEE Transactions on Industry Applications, Vol. 41, pp. 1548–1556, 2005.

[3] M.N. Eskander, "Neural network controller for a permanent magnet generator applied in a wind energy conversion system", Renewable Energy, Vol. 26, pp. 463–477, 2002.

[4] Y.F. Ren, G.Q. Bao, "Control strategy of maximum wind energy capture of direct-drive wind turbine generator based on neural-network", Power and Energy Engineering Conference, pp. 1–4, 2010.

[5] J.S. Thongam, P. Bouchard, R. Beguenane, I. Fofana, "Neural network based wind speed sensorless MPPT controller for variable speed wind energy conversion systems", Electric Power and Energy Conference, pp. 1–6, 2010.

[6] V. Sheeja, P. Jayaprakash, B. Singh, R. Uma, "Neural network theory based voltage and frequency controller for standalone wind energy conversion system", Joint International Conference on Power Electronics, Drives and Energy Systems, pp. 1–6, 2010.

[7] M. Narayana, G. Putrus, "Optimal control of wind turbine using neural networks", Universities Power Engineering Conference, pp. 1–5, 2010.

[8] R. Krishnan, G.H. Rim, "Performance and design of a variable speed constant frequency power conversion scheme with a permanent magnet synchronous generator", Industry Applications Society Annual Meeting, Vol. 1, pp. 45–50, 1989.

[9] O. Ojo, O. Omozusi, "Modeling and analysis of an interior permanent-magnet DC-DC converter generator system", Power Electronics Specialists Conference, Vol. 2, pp. 929–935, 1997.

[10] N. Yamamura, M. Ishida, T. Hori, "A simple wind power generating system with permanent magnet type synchronous generator", International Conference on Power Electronics and Drive Systems, Vol. 2, pp. 849–854, 1999.

[11] Y. Higuchi, N. Yamamura, M. Ishida, T. Hori, "An improvement of performance for small-scaled wind power generating system with permanent magnet type synchronous generator", Industrial Electronics Society, Vol. 2, pp. 1037–1043, 2000.

[12] M.J. Ryan, R.D. Lorenz, "A 'power-mapping' variable-speed control technique for a constant-frequency conversion system powered by a IC engine and PM generator", Industry Applications Conference, Vol. 4, pp. 2376–2382, 2000.

[13] K. Amei, Y. Takayasu, T. Ohji, M. Sakui, "A maximum power control of wind generator system using a permanent magnet synchronous generator and a boost chopper circuit", Power Conversion Conference, Vol. 3, pp. 1447–1452, 2002.

[14] A. Mirecki, X. Roboam, F. Richardeau, "Comparative study of maximum power strategy in wind turbines", International Symposium on Industrial Electronics, Vol. 2, pp. 993–998, 2004.

[15] M. Matsui, X. Dehong, K. Longyun, Z. Yang, "Limit cycle based simple MPPT control scheme for a small sized wind turbine generator system-principle and experimental verification", Power Electronics and Motion Control Conference, Vol. 3, pp. 1746–1750, 2004.

[16] S. Morimoto, H. Kato, M. Sanada, Y. Takeda, "Output maximization control for wind generation system with interior permanent magnet synchronous generator", Industry Applications Conference, Vol. 1, pp. 503–510, 2006.

[17] I. Schiemenz, M. Stiebler, "Control of a permanent magnet synchronous generator used in a variable speed wind energy system", Electric Machines and Drives Conference, pp. 872–877, 2001.

[18] T. Senjyu, S. Tamaki, N. Urasaki, K. Uezato, T. Funabashi, H. Fujita, "Wind velocity and position sensorless operation for PMSG wind generator", 5th International Conference on Power Electronics and Drive Systems, Vol. 1, pp. 787–792, 2003.

[19] M. Chinchilla, S. Arnaltes, J.C. Burgos, "Control of permanent-magnet generators applied to variable-speed wind-energy systems connected to the grid", IEEE Transactions on Energy Conversion, Vol. 21, pp. 130–135, 2006.

[20] A.J.G. Westlake, J.R. Bumby, E. Spooner, "Damping the power-angle oscillations of a permanent-magnet synchronous generator with particular reference to wind turbine applications", Electric Power Applications, Vol. 143, pp. 269–280, 1996.

[21] N. Urasaki, T. Senjyu, K. Uezato, T. Funabashi, H. Fujita, "High efficiency drive for micro-turbine generator based on current phase and revolving speed optimization", 5th International Conference on Power Electronics and Drive Systems, Vol. 1, pp. 737–742, 2003.

[22] M. Kesler, M. Karabacak, E. Özdemir, "Genel amaçlı tristör sürücü eğitim setinin tasarımı ve uygulaması", Otomasyon Dergisi, Vol. 225, pp. 298–304, 2011 (in Turkish).

[23] K. Tan, S. Islam, "Optimum control strategies in energy conversion of PMSG wind turbine system without mechanical sensors", IEEE Transactions on Energy Conversion, Vol. 19, pp. 392–399, 2004.

[24] A. Karakaya, E. Karakas, "Performance analysis of PM synchronous motors using fuzzy logic and self-tuning fuzzy PI speed controls", Arabian Journal for Science and Engineering, Vol. 33, pp. 153–177, 2008.